

# Quartz Crystal Microbalance Studies on Conformational Change of Polymer Chains at Interface

Guangzhao Zhang,\* Chi Wu

The conformation of polymers at interface profoundly influences the interfacial properties. Quartz crystal microbalance with dissipation (QCM-D) is a newly developed technique to detect polymer behavior at interface in real time. In this article, we mainly review our QCM-D studies. Our focus is on temperature induced collapse and swelling of tethered polymer chains, pancake-to-brush transition and mushroom-to-brush of polymer chains.



## Introduction

Polymer chains at interface exhibit rich conformations depending on the polymer structure, grafting density, solvent quality, and polymer segment-surface interaction.<sup>[1–5]</sup> At a low grafting density, if polymer segment attractively interact with the surface, the chains usually exhibit a pancake-like conformation. In contrast, if the segment-surface interaction is non-attractive, the chains have a mushroom structure. At a high grafting density, as the result of the balance between segment-segment repulsion and elasticity of the chains, the chains are stretched away and form brushes. For polyelectrolyte chains, the conformation is also influenced by the charging.

The conformation of polymer chains at interface profoundly influences the interfacial properties such as hydrophilicity, hydrophobicity, adsorption and adhesion. It is imperative that we understand the conformational behavior so that we can tailor the interfacial properties.

However, to study the polymer chains at interface in situ or real time is difficult because the detection methods are scarce. Recently, quartz crystal microbalance with dissipation (QCM-D) has been developed.<sup>[6]</sup> In principle, such a technique can detect the adsorption, conformation and interactions of macromolecules at interface.<sup>[7–14]</sup> This short review deals with the QCM-D studies on conformational change of polymer chains. Due to the limited space, we intend to mainly review what has been done in this laboratory though other research groups have done excellent work in this field.

## QCM-D Measurements

QCM-D and the AT-cut quartz crystal with a fundamental resonant frequency of 5 MHz and a diameter of 14 mm were from Q-sense AB.<sup>[6]</sup> The quartz crystal was mounted in a fluid cell with one side exposed to the solution. The constant ( $C$ ) of the crystal used was  $17.7 \text{ ng} \cdot \text{cm}^{-2} \cdot \text{Hz}$ . The frequency shift was measurable to within  $\pm 1 \text{ Hz}$  in aqueous medium. The effects of surface roughness were minimized by using highly polished crystals with the root mean-square roughness less than 3 nm.<sup>[15]</sup>

When a quartz crystal is excited to oscillate in the thickness shear mode at its fundamental resonant frequency ( $f_0$ ) by applying a RF voltage across the electrodes near the resonant frequency, a small layer

G. Zhang, C. Wu

Hefei National Laboratory for Physical Sciences at Microscale,  
Department of Chemical Physics, University of Science and  
Technology of China, Hefei, China

E-mail: gzzhang@ustc.edu.cn

C. Wu

Department of Chemistry, The Chinese University of Hong Kong,  
Shatin, N.T., Hong Kong, China



**Guangzhao Zhang** received his BS and PhD from Chengdu University of Science and Technology and Fudan University, respectively. He is currently a Professor in the Department of Chemical Physics at University of Science and Technology of China. Currently, he works on polymer solutions, polymeric interfaces and intermolecular interactions.



**Chi Wu** was born in Wuhu, Anhui, China (1955). He was educated at the University of Science and Technology of China (B.Sc., 1982) and the State University of New York at Stony Brook (Ph.D., 1987) and is currently Professor of Chemistry at Chinese University of Hong Kong. His scientific interests cover various aspects of polymer physics and colloidal chemistry, particularly design, synthesis and assembly of functional macromolecules, development of non-viral vectors for molecular medicines, dynamics and interaction of macromolecules in solution, structures and dynamics of polymer gel networks, characteristic properties of special intractable polymers.

added to the electrodes induces a decrease in resonant frequency ( $\Delta f$ ) which is proportional to the mass ( $\Delta m$ ) of the layer. In vacuum or air, if the added layer is rigid, evenly distributed and much thinner than the crystal, the  $\Delta f$  is related to  $\Delta m$  and the overtone number ( $n = 1, 3, 5, \dots$ ) by the Sauerbrey equation,<sup>[16]</sup>

$$\Delta m = -\frac{\rho_q l_q \Delta f}{f_0 n} \quad (1)$$

where  $f_0$  is the fundamental frequency,  $\rho_q$  and  $l_q$  are the specific density and thickness of the quartz crystal, respectively. The dissipation factor is defined by

$$\Delta D = \frac{E_d}{2\pi E_s} \quad (2)$$

where  $E_d$  is the energy dissipated during one oscillation and  $E_s$  is the energy stored in the oscillating system. The measurement of  $\Delta D$  is based on the fact that the voltage over the crystal decays exponentially as a damped sinusoidal when the driving power of a piezoelectric oscillator is switched off.<sup>[6]</sup> By switching the driving voltage on and off periodically, we can simultaneously obtain a series of the changes of the resonant frequency and the dissipation factor.

In a Newtonian liquid, the frequency response of a quartz resonator can be quantitatively described by the Kanazawa-Gordon relation,<sup>[17]</sup>

$$\Delta f = -n^{0.5} f_0^{1.5} (\eta_l \rho_l / \pi \mu_q \rho_q)^{0.5} \quad (3)$$

where  $f_0$  is the fundamental frequency,  $n$  is the harmonic number,  $\rho_q$  and  $\mu_q$  are the density and shear modulus of

quartz,  $\rho_l$  and  $\eta_l$  are the density and viscosity of the liquid medium, respectively. The dissipation response is given by,<sup>[18,19]</sup>

$$\Delta D = 2(f_0/n)^{0.5} (\eta_l \rho_l / \pi \mu_q \rho_q)^{0.5} \quad (4)$$

The frequency and dissipation responses due to the grafting of the polymer chains on the surface of the quartz resonator can be obtained by removing the effects of the viscosity and density of water based on Equation (3) and (4).  $\Delta f$  and  $\Delta D$  values from the fundamental were usually noisy because of insufficient energy trapping and thus discarded.<sup>[20]</sup>

### Temperature Induced Conformational Change of Poly(*N*-isopropylacrylamide) (PNIPAM) Mushroom

PNIPAM is a well-known thermally sensitive polymer and has a lower critical solution temperature (LCST) at  $\approx 32^\circ\text{C}$  in water.<sup>[21]</sup> It is well established that PNIPAM chains swell at a temperature below LCST with a random coil conformation but collapse into globules at a temperature above LCST.<sup>[22]</sup> For PNIPAM chains grafted on surface, the conformational change is still an open question. Some studies demonstrate that PNIPAM chains have a sharp transition near the LCST,<sup>[23,24]</sup> but recent investigations indicate a gradual collapse.<sup>[25]</sup> The latter agrees with the prediction.<sup>[4,5]</sup> To clarify the question, we have prepared thiol-terminated PNIPAM (HS-PNIPAM) ( $\bar{M}_w = 11\,800\text{ g}\cdot\text{mol}^{-1}$ ,  $\bar{M}_w/\bar{M}_n = 1.24$ ) and investigated the collapse and swelling of the chains grafted on gold surface. Because the chains are prepared by the "grafting to" procedure and the grafting time is short, the chains have a low grafting density and only form mushrooms.<sup>[10]</sup>

Figure 1 shows the temperature dependence of the frequency shift ( $\Delta f$ ). During the heating process, as temperature increases,  $-\Delta f$  decreases. Based on Equation

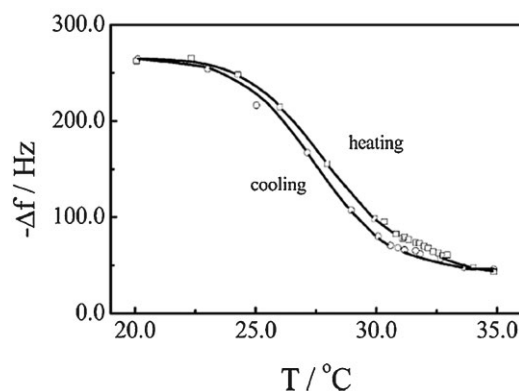


Figure 1. Temperature dependence of frequency change ( $\Delta f$ ) of PNIPAM mushroom on gold surface.

(1), we know that the mass of the layer on the sensor surface decreases with temperature. Note that the mass here includes the mass of the grafted polymer chains and that of the water molecules bound on the chains, so we called it hydrodynamic mass. Since PNIPAM chains are grafted on the surface, the decrease in mass is due to the dehydration, that is, some bounded water molecules leave the PNIPAM layer. During the cooling process,  $-\Delta f$  increases with decreasing temperature, indicating that hydration increases as temperature decreases. Eventually,  $-\Delta f$  is back to the original point because PNIPAM chains resume complete hydration.

Figure 2 shows the temperature dependence of the dissipation ( $\Delta D$ ). It is known that dissipation of a viscoelastic polymer layer on quartz resonator is substantially influenced by its structure. A dense or rigid layer has a small dissipation of energy, while a layer with a looser or more flexible structure exhibits a larger dissipation.<sup>[6]</sup> Here,  $\Delta D$  decreases with temperature during the heating process, indicating that PNIPAM chains shrink and collapse into a denser structure. During the cooling process,  $\Delta D$  increases with the decreasing temperature, indicating the swelling of PNIPAM chains. In addition, Figure 1 and 2 show a hysteresis in the heating-and-cooling cycle. This is because PNIPAM segments form additional hydrogen bonds at the collapsed state, which cannot be completely removed at a temperature near LCST.<sup>[22]</sup>

Figure 3 shows the  $\Delta D$  vs  $\Delta f$  relation. Since  $\Delta f$  mainly arises from the dehydration or hydration of polymer chains whereas  $\Delta D$  is due to the conformation change,  $\Delta D$  vs  $\Delta f$  relation can describe the cooperativity between the conformation and solvation of polymer chains. The fact that  $\Delta D$  linearly increases with  $-\Delta f$  indicates that the conformational change involves only one kinetic process. Thus, the dehydration and collapse occur simultaneously,

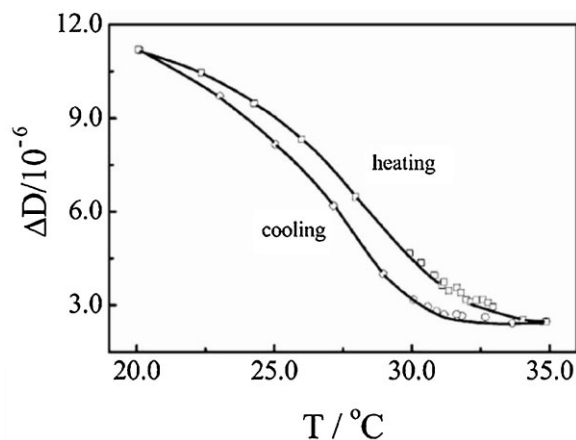


Figure 2. Temperature dependence of dissipation change ( $\Delta D$ ) of PNIPAM mushroom on gold surface.

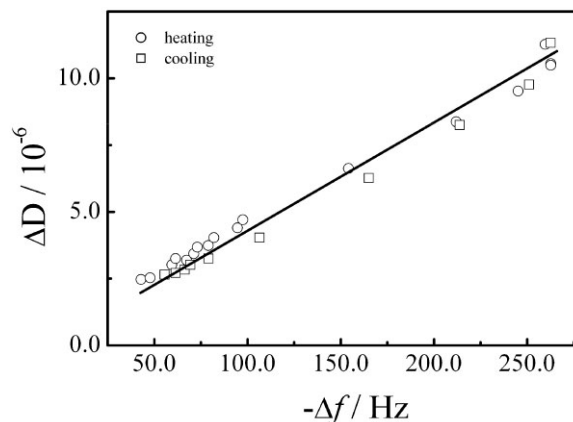


Figure 3.  $\Delta D$  vs  $\Delta f$  relation for PNIPAM mushroom on gold surface.

and the hydration is concurrent with the swelling. Namely, they have strong cooperativity.

#### Temperature Induced Conformational Change of PNIPAM Brush

We have also investigated temperature induced conformational change of PNIPAM brushes.<sup>[11]</sup> By anchoring initiator molecules on  $\text{SiO}_2$ -coated resonator surface, PNIPAM chains ( $\bar{M}_w = 9.3 \cdot 10^5 \text{ g} \cdot \text{mol}^{-1}$ ,  $\bar{M}_w/\bar{M}_n = 2.0$ ) grow from the surface. Such chains prepared by the "grafting from" procedure have a higher grafting density and form polymer brushes. Figure 4 shows the temperature dependence of frequency shift ( $-\Delta f$ ) of the brush in one heating-and-cooling cycle. Like the case in PNIPAM mushroom, as temperature increases,  $-\Delta f$  gradually decreases in the heating process due to the chain dehydration. During the cooling process, the collapsed PNIPAM brush becomes swollen with decreasing temperature reflecting in the increase of  $-\Delta f$ .

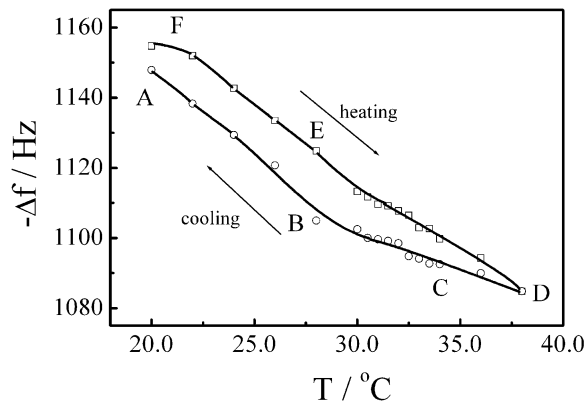


Figure 4. Temperature dependence of frequency change ( $\Delta f$ ) of PNIPAM brush on  $\text{SiO}_2$  surface.

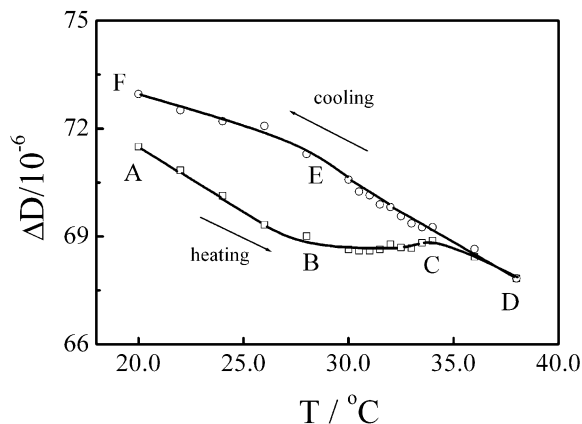


Figure 5. Temperature dependence of dissipation change ( $\Delta D$ ) of PNIPAM brush on  $\text{SiO}_2$  surface.

Figure 5 shows  $\Delta D$  decreases with the increasing temperature in the heating process indicating that PNIPAM brush gradually collapses into a more compact structure. Nevertheless, there is an observed transition at  $\approx 34^\circ\text{C}$ . During the cooling process, the dissipation smoothly increases with the decreasing temperature over the range of temperature from 38 to  $20^\circ\text{C}$ , indicating that the collapsed brush becomes more swollen and flexible. However, no transition can be observed in the cooling process. Figure 5 also shows that the  $\Delta D$  value during the cooling process is generally larger than that during heating process at the same temperature, whereas an opposite trend is found for  $\Delta f$  data shown in Figure 4. The phenomenon can be attributed to the tails on the outer layer of the brush, which have critical effects on the dissipation. During the heating process, PNIPAM chains collapsing from the stretching state do not have a chance to produce flexible and random tails. During the cooling process, the brush swells from the outer layer to inner core resulting in some swollen tails which behave like short chains tethered on the inner layer. At the initial stage, since the distance between the tails is not short enough, no stretching occurs. Accordingly, the random and flexible tails give rise to a marked increase of  $\Delta D$  further smoothing the transition. On the other hand, because the amount of water molecules coupled to the tails is limited,  $-\Delta f$  increases a little. Further cooling leads the segments of PNIPAM near the sensor surface to be swollen and the distance between tails increase, so that the tails would stretch. Actually, we found that it took about one week for PNIPAM brushes to completely swell at  $20^\circ\text{C}$ . During the time for the QCM-D experiment, the tails did not completely stretch yet. This can be confirmed by the facts that both  $\Delta D$  and  $\Delta f$  were not back to their original values at  $20^\circ\text{C}$  (Figure 4 and 5).

Figure 4 and 5 clearly indicate that PNIPAM chains undergo a continuous transition. Such a transition has

been predicted by theory<sup>[3,4]</sup> and observed in some experiments.<sup>[25,26]</sup> The continuity has been attributed to the high density and non-uniformity of the chains, which lead to a spectrum of the collapse rates.<sup>[1–3]</sup> The surface constraint can also broaden the transition.<sup>[4]</sup> Note that the collapse of a polymer brush has been predicted to be accompanied by a solubility transition,<sup>[5,7]</sup> the cooperativity of the two transitions can also influence the continuity. The effects of cooperativity on the volume change of some hydrogels<sup>[27]</sup> and DNA condensation<sup>[28]</sup> have been reported. However, because the collapse and solubility transitions are difficult to separate in experiment, such cooperativity effect is still poorly understood. As discussed above,  $\Delta f$  is mainly caused by the dehydration or hydration, while  $\Delta D$  is due to the conformational change. The relation between  $\Delta D$  and  $\Delta f$  can provide useful information about the cooperativity and the kinetics of the collapse transition.

Figure 6 clearly reveals three kinetic processes in the heating process. When  $T < 28^\circ\text{C}$  (A to B),  $\Delta D$  decreases with  $-\Delta f$  decreasing, implying that the shrinking and dehydration of PNIPAM chains happen simultaneously. In the range  $28^\circ\text{C} < T < 34^\circ\text{C}$  (B to C),  $\Delta D$  slightly change as  $-\Delta f$  decreases. Like individual PNIPAM chains,<sup>[22]</sup> PNIPAM brush partially collapses in this range of temperature so that  $\Delta D$  exhibits a small change. On the other hand, not all the detached water molecules during shrinking at  $T < 28^\circ\text{C}$  can leave PNIPAM brushes immediately, some of them are trapped in the dense brush. As temperature increases, the trapped water molecules gradually diffuse out of the brush leading to a frequency change. Obviously, the cooperativity between the collapse and dehydration is weak due to the retarded dehydration. This also leads the collapse transition to be more continuous. Further heating overcomes the energy barrier for the stretching so that the brush is dehydrated and collapse again reflecting in the decreases of  $\Delta D$  and  $-\Delta f$  at  $T > 34^\circ\text{C}$  (C to D). During the

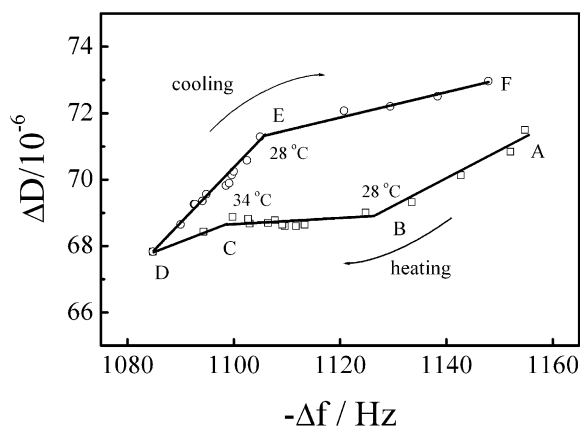


Figure 6.  $\Delta D$  vs  $\Delta f$  relation for PNIPAM brush on  $\text{SiO}_2$  surface.

cooling process, at a temperature above 28 °C (D to E),  $\Delta D$  rapidly increases as  $-\Delta f$  increases, suggesting that the tails on outer layer are hydrated and flexible. At  $T < 28$  °C (E to F),  $\Delta D$  slows down its increase because the hydrated chains in the outer layer tend to stretch and pack more densely. Note that for the same  $-\Delta f$ , the  $\Delta D$  value during the cooling process is always higher than that during the heating process, further indicating that the flexible tails have pronounced an effect on the dissipation.

Figure 4, 5 and 6 also show a hysteresis in one heating-and-cooling cycle, indicating an irreversible collapse transition. For free PNIPAM chains in dilute solution and PNIPAM mushrooms, the hysteresis has been attributed to the intrachain and interchain hydrogen bonding formed in the collapsed state, which hinder the hydration of the collapsed chains during the cooling process. For PNIPAM brush, besides the chain knotting and entanglement formed via the hydrogen bonding, the non-uniformity and the stretching of the brushes would enlarge the hysteresis.

#### Pancake-to-Brush Transition of PNIPAM Chains

We have prepared narrowly-distributed HS-PNIPAM ( $\overline{M}_w = 18\,332 \text{ g} \cdot \text{mol}^{-1}$ ,  $\overline{M}_w/\overline{M}_n = 1.04$ ) by using reversible addition-fragmentation chain transfer (RAFT) polymerization and the subsequent hydrolysis. The chains can be grafted on the gold-coated crystal surface via chemical coupling between thiol groups and gold.<sup>[29]</sup> On the other hand, our experiments indicate the PNIPAM segments can be absorbed on the gold surface due to the segment-surface interaction. Therefore, a pancake-to-brush transition can be achieved in the system. We have investigated the grafting kinetics of the PNIPAM chains from an aqueous solution using QCM-D in real time.<sup>[12]</sup>

Figure 7 shows the frequency shift ( $\Delta f$ ) of the quartz resonator immersed in the aqueous solution of HS-PNIPAM (*s*-PNIPAM) chains as a function of logarithmic time.

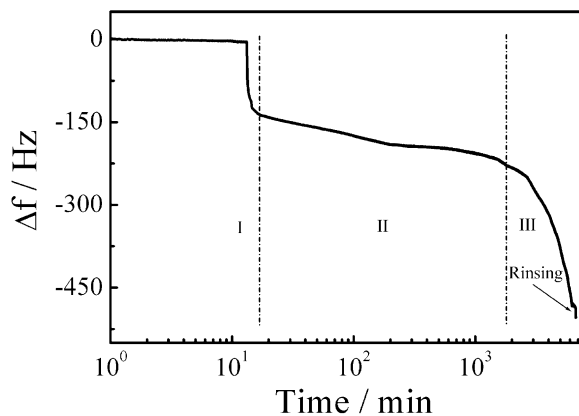


Figure 7. Frequency change ( $\Delta f$ ) of the quartz resonator immersed in *s*-PNIPAM aqueous solution as a function of logarithmic time.

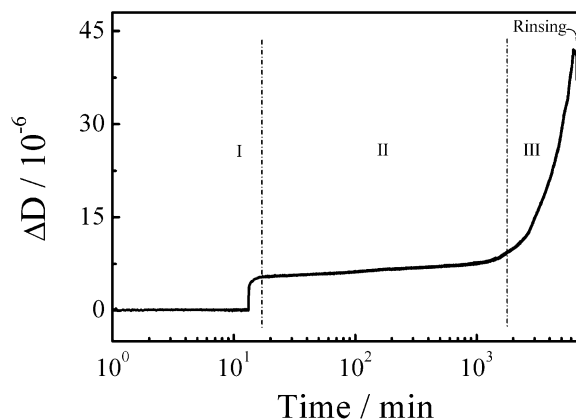
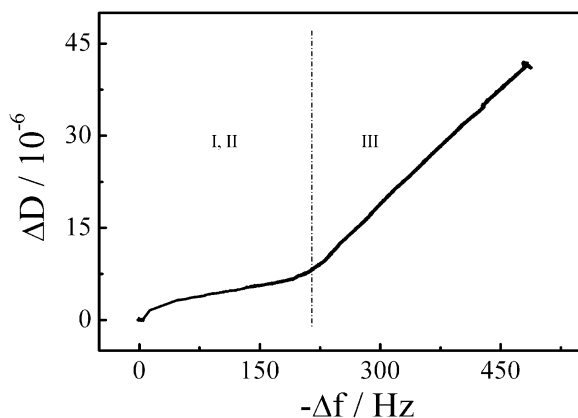


Figure 8. Dissipation change ( $\Delta D$ ) of the quartz resonator immersed in *s*-PNIPAM aqueous solution as a function of logarithmic time.

Clearly, the grafting exhibits a three-regime character. At the initial stage (regime I),  $\Delta f$  significantly decreases indicating that the chains are quickly grafted on the bare gold surface. In regime II, the slow decrease of  $\Delta f$  indicates that the chains are gradually grafted on the surface because the chains already grafted on the surface hinder the grafting of incoming chains. An accelerated grafting occurs in regime III reflecting in the relatively sharp decrease in  $\Delta f$ , suggesting that the conformation of the already grafted chains has changed so that incoming chains can be accommodated.

Figure 8 shows the change of dissipation ( $\Delta D$ ) as a function of logarithmic time. The sharp increase in  $\Delta D$  in regime I further indicates the quick grafting of the chains. In regime II, the slow increase in dissipation indicates a gradual grafting. The large  $\Delta D$  in regime III indicates the acceleration of the grafting and the increase of the thickness of the polymer layer.

The three-regime-grafting has been reported by Penn and coworkers.<sup>[30]</sup> Corresponding to regime I, II and III, grafted chains exhibit the conformation of pancake, mushroom and brush.<sup>[31–33]</sup> As discussed above, PNIPAM chains are not only grafted with their end groups but also adsorbed with their segments on gold surface. At a low grafting density, the chains form a pancake-like structure. In regime II, as the grafting density increases, the uncovered area between the already grafted chains become narrow, the segments of the incoming chains are expected to be partially adsorbed on the surface, other segments would turn up and overlap with the already grafted chains. Since the uncovered area is still enough for accommodating an end group, the grafting would continue though it becomes much slower. Meanwhile, the local segment-segment repulsion has accumulated. When the thiol-gold interaction is dominant over segment-gold interaction, as the result of the balance between



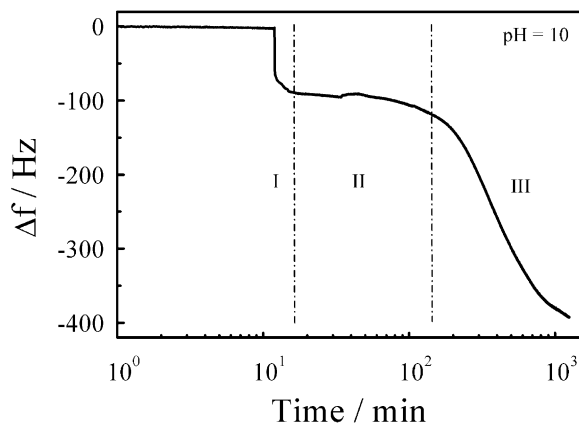
■ Figure 9.  $\Delta D$  vs  $\Delta f$  relation for *s*-PNIPAM on gold surface.

the local segment-segment repulsion and rubber-like elasticity of the chains, the adsorbed segments begin to desorb and protrude from the gold surface forming more loops and tails. Thus, the conformation of the grafted chains transits from a “pancake” to a “mushroom.” After the rearrangement, the space between neighboring chains is large enough to accommodate the incoming chains, which makes the further grafting possible. As the grafting density increases, the grafted chains form brush.

The conformation change of *s*-PNIPAM chains can be clearly viewed in terms of  $\Delta D$  vs  $\Delta f$  relation (Figure 9). The grafting involves two kinetic processes. The same  $\Delta D$  vs  $\Delta f$  relation in regime I and II indicates that there is not much difference between the chain conformations in the two regimes. Moreover,  $\Delta D$  gradually increases with  $-\Delta f$  in the two regimes. It is reasonable to ascribe the conformations in regime I and II to a pancake and a mushroom, respectively, because the chains in both conformations are random coils. A much larger slope can be observed in regime III, indicating that the thickness increases with the grafting density much more than that in regime I and II. The grafted chains in regime III have a more stretched conformation, that is, the chains form brushes. Accordingly, the mushroom-to-brush transition occurs from regime II to III.

### Mushroom-to-Brush Transition of Polymer Chains

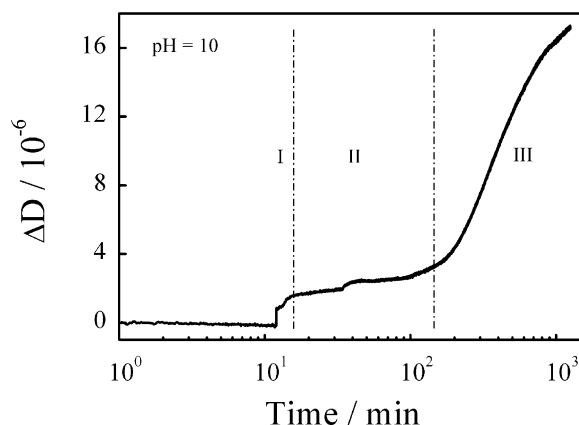
Parallel to the pancake-to-brush transition, we have studied the mushroom-to-brush transition of polymer chains on gold surface by use of narrowly-distributed thiol-terminated poly[(2-dimethylamino)ethyl methacrylate] (HS-PDMEM) ( $\bar{M}_w = 21\,858 \text{ g} \cdot \text{mol}^{-1}$ ,  $\bar{M}_w/\bar{M}_n = 1.17$ ). The sample was prepared via the same procedure for HS-PNIPAM discussed in last section. Our experiments indicate that the interaction between PDEMEM segment and gold surface is very weak in the range pH = 2–10. Thus,



■ Figure 10. Change of frequency ( $\Delta f$ ) of the quartz resonator immersed in HS-PDMEM solution at pH 10 as a function of logarithmic time.

PDMEM chains are expected to form a mushroom instead of a pancake in the initial stage.<sup>[13]</sup>

Figure 10 and 11 respectively show the changes of frequency ( $\Delta f$ ) and dissipation ( $\Delta D$ ) at pH 10 as the function of logarithmic time after HS-PDMEM is introduced. Either  $\Delta f$  or  $\Delta D$  finally reaches a constant indicating the saturation of the gold surface. Clearly, a three-regime-grafting can be observed. At the initial stage, the significant decrease in  $\Delta f$  (regime I) indicates that the chains are quickly grafted on the bare gold surface. Subsequently, the grafting slows down (regime II) due to hindrance of the already grafted chains. Finally, the grafting speeds up reflecting in a relatively sharp decrease of  $\Delta f$  (regime III), indicating that the conformation of the already grafted chains has changed so that the incoming chains can be grafted again. The quick increase in  $\Delta D$  in regime I further indicates the grafting of the chains, whereas the slight increase of  $\Delta D$  in regime II indicates slight grafting occurs. The large  $\Delta D$  in regime III indicates a thick layer.



■ Figure 11. Change of dissipation ( $\Delta D$ ) of the quartz resonator immersed in HS-PDMEM solution at pH 10 as a function of logarithmic time.

The three-regime grafting has also been observed at pH 6 and pH 2. However, the span for regime II decreases with the degree of charging of the grafted chains.<sup>[13]</sup> As we know, the chains are quickly and randomly tethered on the gold surface in regime I leading to some local overlapping of the chains because the grafting is controlled by the centre-of-mass diffusion. Driven by the balance between the local segment-segment repulsion and elasticity of the chains, the locally overlapped chains tend to eliminate the overlapping, and thus make a rearrangement themselves in regime II. Since PDMEM has  $pK_a = 6.6$ , the chains are uncharged, partially charged and completely charged at pH 10, 6 and 2, respectively.<sup>[34]</sup> As the degree of charging increases, the electrostatic repulsion between the chains becomes strong, and the local overlapping is difficult. This explains that the time for the rearrangement decreases with the degree of charging. Our results indicate that conformation of the grafted chains in regime II is slightly different from that in regime I, i.e., the chains form a “random” mushroom in regime I but a “ordered” mushroom in regime II. The latter without local chain overlapping makes further grafting possible. After the rearrangement, the space between two neighbor chains is enough to accommodate incoming chains.

In regime III, the grafting through the ordered mushroom structure proceeds until saturation is reached. The marked changes in frequency and dissipation from regime II to regime III suggest that the grafted chains form a structure much different from the mushroom structure in regime I and II, or the chains form brushes in regime III. The gradual decrease in  $\Delta f$  and increase in  $\Delta D$  with time in regime III indicate that the grafting density increases and the chains become stretched. In addition, the frequency shift ( $\Delta f_s$ ) and dissipation factor ( $\Delta D_s$ ) at saturation decrease with the degree of charging. This is because an incoming chain must keep its distance from an already grafted chain so that it can be grafted. A strong repulsion

leads to a large distance or a small grafting density. Accordingly,  $\Delta f_s$  and  $\Delta D_s$  decrease with the degree of charging.<sup>[13]</sup>

Figure 12 shows that the grafting involves two kinetic processes. Such a character can also be observed at pH 6 and 2. The same  $\Delta D$  vs  $\Delta f$  relation in regime I and II further indicates only a minor difference between the chain conformations in the two regimes. In other words, the chains form a mushroom in the two regimes. In regime III, a quite different kinetic process can be observed, indicating that the grafted chains have a conformation different from that in regime I and II, namely, they form brushes. Accordingly, the mushroom-to-brush transition occurs from regime II to regime III.

## Summary and Outlook

QCM-D is effective to characterize conformational change of polymer chains at an interface. For polymer chains grafted at a solid-liquid interface, the dehydration and hydration can be described by frequency shift ( $\Delta f$ ), whereas the collapse and swelling are related to the dissipation change ( $\Delta D$ ).  $\Delta f$  vs  $\Delta D$  can describe the cooperativity between dehydration (hydration) and collapse (swelling). QCM-D can detect the grafting kinetics of polymer chains on solid-liquid interface in real time. The pancake-to-brush and mushroom-to-brush transition can be observed from the changes in frequency ( $\Delta f$ ) and dissipation ( $\Delta D$ ).

**Acknowledgements:** The financial support of the *National Natural Scientific Foundation of China* (NNSFC) Projects (20725414 and 20574065), the *Ministry of Science and Technology of China* (2007CB936401) and the *Hong Kong Special Administration Region* (HKSAR) Earmarked Project (CUHK4036/05P, 2160269) is gratefully acknowledged.

Received: September 29, 2008; Accepted: November 3, 2008; DOI: 10.1002/marc.200800611

**Keywords:** conformation; grafting kinetics; interface; polymer brush; quartz crystal microbalance

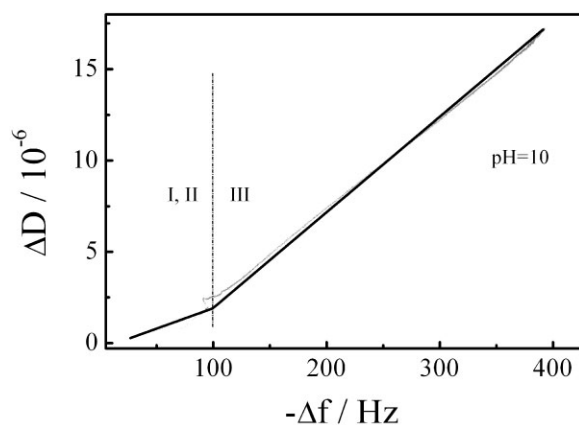


**Figure 12.**  $\Delta D$  vs  $\Delta f$  relation for HS-PDMEM on gold surface at pH 10.

- [1] S. Alexander, *J. Phys. Fr.* **1977**, *38*, 983.
- [2] P. G. de Gennes, *Macromolecules* **1980**, *13*, 1069.
- [3] S. T. Milner, *Science* **1991**, *251*, 905.
- [4] E. B. Zhulina, O. V. Borisov, V. A. Pryamitsyn, T. M. Birshtein, *Macromolecules* **1991**, *24*, 140.
- [5] A. Halperin, M. Tirrell, T. P. Lodge, *Adv. Polym. Sci.* **1992**, *100*, 31.
- [6] [6a] M. Rodahl, F. Höök, A. Krozer, B. Kasemo, P. Brezinsky, *Rev. Sci. Instrum.* **1995**, *66*, 3924; [6b] M. V. Voinova, M. Rodahl, M. Jonson, B. Kasemo, *Phys. Scrip.* **1999**, *59*, 391.
- [7] F. Höök, M. Rodahl, P. Brezinski, B. Kasemo, P. Brezinski, *Proc. Natl. Acad. Sci. U. S. A.* **1998**, *95*, 12271.

- [8] [8a] S. Moya, O. Azzaroni, T. Farhan, V. L. Osborne, W. T. S. Huck, *Angew. Chem. Int. Ed.* **2005**, *44*, 4578; [8b] S. E. Moya, A. A. Brown, O. Azzaroni, W. T. S. Huck, *Macromol. Rapid Commun.* **2005**, *26*, 1117.
- [9] Y. K. Jhon, R. R. Bhat, C. Jeong, O. J. Rojas, I. Szleifer, J. Genzer, *Macromol. Rapid Commun.* **2006**, *27*, 697.
- [10] G. Z. Zhang, *Macromolecules* **2004**, *37*, 6553.
- [11] G. M. Liu, G. Z. Zhang, *J. Phys. Chem. B* **2005**, *109*, 743.
- [12] G. M. Liu, H. Cheng, L. F. Yan, G. Z. Zhang, *J. Phys. Chem. B* **2005**, *109*, 22603.
- [13] G. M. Liu, L. F. Yan, X. Chen, G. Z. Zhang, *Polymer* **2006**, *47*, 3157.
- [14] G. M. Liu, G. Z. Zhang, *Langmuir* **2005**, *21*, 2086.
- [15] L. Daikhin, M. Urbakh, *Faraday Discuss.* **1997**, *107*, 27.
- [16] G. Z. Sauerbrey, *Phys.* **1959**, *155*, 206.
- [17] K. Z. Kanazawa, J. G. Gordon III, *Anal. Chem.* **1985**, *57*, 1770.
- [18] C. D. Stockbridge, "Resonance Frequency vs. Mass Added to Quartz Crystals", in: *Vacuum Microbalance Techniques*, M. J. Katz, Ed., Plenum Press, New York 1966.
- [19] M. Rodahl, B. Kasemo, *Sens. Actuators A* **1996**, *54*, 448.
- [20] V. E. Bottom, "Introduction to Quartz Crystal Unit Design", Van Nostrand Reinhold Co., New York 1982.
- [21] M. Heskins, J. E. Guillet, E. James, *J. Macromol. Sci., Chem.* **1968**, *A2*, 1441.
- [22] [22a] C. Wu, S. Zhou, *Macromolecules* **1995**, *28*, 5388; [22b] C. Wu, S. Zhou, *Phys. Rev. Lett.* **1996**, *77*, 3053; [22c] C. Wu, X. H. Wang, *Phys. Rev. Lett.* **1998**, *80*, 4092.
- [23] Y. G. Takei, T. Aoki, K. Sanui, N. Ogata, Y. Sakurai, T. Okano, *Macromolecules* **1994**, *27*, 6163.
- [24] J. Zhang, R. Pelton, Y. Deng, *Langmuir* **1995**, *11*, 2301.
- [25] S. Balamurugan, S. Mendez, S. S. Balamurugan, M. J. O'Brien II, G. Z. Lopez, *Langmuir* **2003**, *19*, 2545.
- [26] A. Domack, S. Prucker, J. Rühle, D. Johannsmann, *Phys. Rev. E* **1997**, *56*, 680.
- [27] M. Annaka, K. Motokawa, S. Sasaki, T. Nakahira, H. Kawasaki, H. Maeda, Y. Arno, Y. Tominaga, *J. Chem. Phys.* **2000**, *113*, 5980.
- [28] T. Iwataki, K. Yoshikawa, S. Kidoaki, D. Umeno, M. Kiji, M. Maeda, *J. Am. Chem. Soc.* **2000**, *122*, 9891.
- [29] J. C. Love, L. A. Estroff, J. K. Kriebel, R. G. Nuzzo, G. M. Whitesides, *Chem. Rev.* **2005**, *105*, 1103.
- [30] [30a] L. S. Penn, T. F. Hunter, Y. Lee, R. P. Quirk, *Macromolecules* **2000**, *33*, 1105; [30b] L. S. Penn, H. Huang, M. D. Sindkhedkar, S. E. Rankin, K. Chittenden, R. P. Quirk, R. P. Mathers, Y. Lee, *Macromolecules* **2002**, *35*, 7054; [30c] H. Huang, L. S. Penn, R. P. Quirk, T. H. Cheong, *Macromolecules* **2004**, *37*, 516; [30d] H. Huang, S. E. Rankin, L. S. Penn, R. P. Quirk, T. H. Cheong, *Langmuir* **2004**, *20*, 5770.
- [31] T. R. Baekmark, G. Elender, D. D. Lasic, E. Sackmann, *Langmuir* **1995**, *11*, 3975.
- [32] T. R. Baekmark, T. Wiesenthal, P. Kuhn, A. Albersdörfer, O. Nuyken, R. Merkel, *Langmuir* **1999**, *15*, 3616.
- [33] T. Wiesenthal, T. R. Baekmark, R. Merkel, *Langmuir* **1999**, *15*, 6837.
- [34] A. S. Lee, A. P. Gast, V. Bütün, S. P. Armes, *Macromolecules* **1999**, *32*, 4302.